Review of probabilistic methods for dynamic stability of ships in rough seas

Clève Wandji, *Bureau Veritas,* cleve.wandji@bureauveritas.com

ABSTRACT

This paper is focused on reviewing some probabilistic methods to evaluate dynamic stability event (for example large roll angle or large acceleration). In order to analyze the assumptions behind these methods and to identify the link between them, these different statistical methodologies will be tested in two datasets obtained by numerical simulations. The first dataset represents a nonlinear process (parametric roll condition) and the second a linear process. Both processes are obtained from a very long simulation 3000 hours (3h x 1000) in order to insure a better statistical convergence of the sampling. In addition, when possible, a Pearson chi-square test goodness of fit will be performed to determine whether there is a significant difference between the expected data and the observed data.

Keywords: *Probabilistic methods, nonlinear process, direct stability assessment, independence of events, Chi-square test.*

1. INTRODUCTION

Predicting the stability of a ship in waves is quite an important and challenging problem as recognized by the International Maritime Organization (IMO). The generalized problem of stability in waves has been subdivided into five stability failure modes, which are: parametric rolling, pure loss of stability, surf-riding/broaching, loss of stability under dead ship condition and excessive accelerations (Wandji and Corrignan 2012). Note that the Ship Design and Construction IMO Sub-Committee is developing the Second Generation Intact Stability Criteria (SGISC) for these five stability failure modes. These SGISC are based on a multi-tiered assessment approach. The third level also called direct stability assessment used probability for the definition of the criteria and also for the safety level.

Difficulties to evaluate probability of large event (roll angles and accelerations) are related to both the rarity of the event and the nonlinearities of the dynamical system describing ship behavior in rough seas. These nonlinearities are due to stiffness, roll damping, excitation for example, and since they are essential to properly model these phenomena, alternatives for accurate assessment may be limited to numerical simulations (for example using potential code for parametric roll) and model test. These stability failure modes are caused by irregular waves and/or gusty wind, and the inherent randomness of these environmental conditions makes the use of the probability of stability failure a very useful tool for both design and operation.

In order to test and understand the assumptions behind the different methodologies, an example has been generated and used for different probabilistic approaches. These approaches are discussed in this study. The present work is subdivided in the main following parts: first of all, the example case generated to test different methodologies will be presented; secondly, definitions of different statistics used in this work and their application on a linear process and a nonlinear process are presented; and finally the link between these different statistics are discussed.

2. EXAMPLE CASE

The roll motion time series has been obtained by performing time domain simulation on C11 containership. The main characteristics of this vessel are contained in Table 1 and a body plan is shown in Figure 1.

Simulations conditions

Nonlinear time domain computations using HydroStar++ (see Wandji C. (2018) for more details on this tool) have been performed in following, irregular and short crested seas having Hs = 6m and Tp = 12.5s. For this sea state, 1000 realizations have been computed. For each realization a different set of random phases, frequencies of the wave component composing the sea state is used.

Table 1: Main characteristics of C11 containership

Parameter	Value	Unit
Length between perpendiculars	262.0	m
Breath	40.0	m
Speed	0.0	m/s
Natural roll period	25.1	s
Metacentric height	2.75	m
Bilge keel length	76.28	m
Bilge keel breath	0.4	m

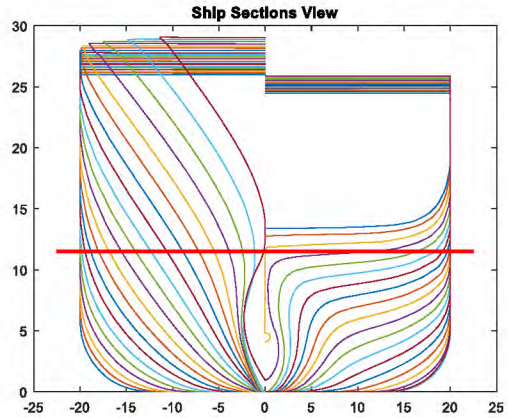

Figure 1: Body plan of C11 containership.

The ship experiences large roll motions in almost all realizations which can be related in this case to parametric rolling, since we are in following waves and the natural roll period is about twice the encounter period. An example of roll motion time series for one realization is shown in Figure 2 (blue line). Note that this signal can be considered as a nonlinear process since parametric rolling is a highly nonlinear phenomenon.

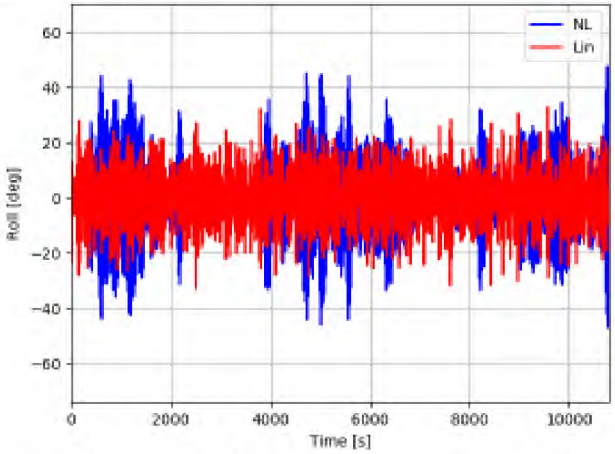

Figure 2: Time series for nonlinear (parametric roll, blue line) and linear processes (red line) for 3h.

Construction of the linear process

Using the 1000 simulations (3000 hours = 3 hours x 1000) for the nonlinear process, a power spectral density has been built, afterward the linear process has been generated. Thus the nonlinear and linear processes have the same energy content. Figure 3 shows the two spectrums derived from the two processes, they are identical. Figure 2 shows an example of time series for one realization of 3 hours for both processes.

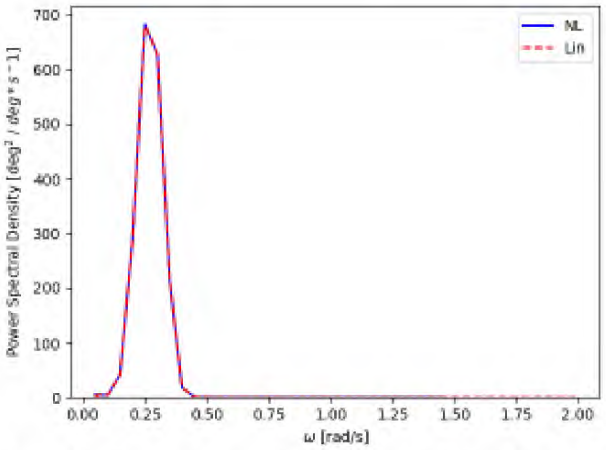

Figure 3: Power spectral density for nonlinear (blue) and linear (red) processes.

Using the two processes (linear and nonlinear) defined above, we will review, define and test some available formulations for connecting the probability of occurrence (large roll angle or accelerations for example) and the time of exposure. In this paper, all results for the linear process will be represented in red and those for the nonlinear process in blue.

3. DISTRIBUTION OF INSTANTANEOUS VALUES

Instantaneous value distribution is the distribution of the process itself at each instant of time, for example for our example case the instantaneous value distribution will be the distribution of roll angle at any instant of time. For a linear process x (for example roll angle), with standard deviation σ_x, it is known that the instantaneous value distribution F_i follows a Gaussian or Normal distribution with zero mean:

$$F_i = \phi\left(\frac{x}{\sigma_x}\right) \quad (1)$$

Note that ϕ is the standard normal distribution (with zero mean and unit variance). Using the linear and nonlinear processes presented in section 2 the instantaneous value distribution have been computed and the results are shown in Figure 4 (probability density function) and Figure 5 (exceedance probability). As expected, the linear

process follows very well the theoretical distribution (named Gauss in Figure 4 and Figure 5), while the nonlinear process has an unknown shape.

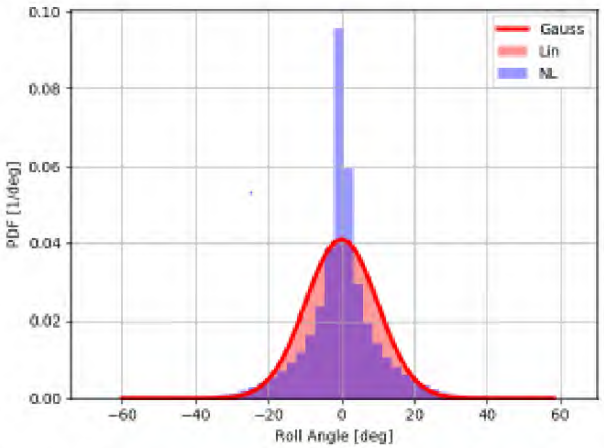

Figure 4: Probability density function of the instantaneous value distribution.

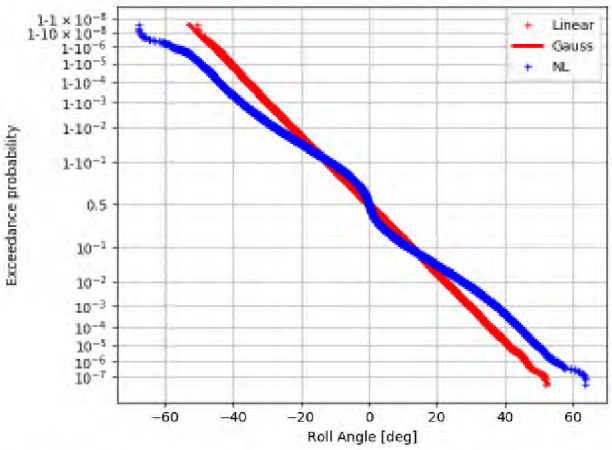

Figure 5: Instantaneous value distribution for linear and nonlinear processes.

4. UPCROSSING RATE DISTRIBUTION

Using the crossing theory, the upcrossing rate ν of a process x can be found using equation (2) under the condition that the process is differentiable with $\dot{x}$ being the time derivative of the process x.

$$\frac{dp}{dt} = \int_0^\infty f(x,\dot{x})\dot{x}d\dot{x} = \nu\big(x(t)\big) \qquad (2)$$

The integral in formula (2) has also the meaning of derivative of the instantaneous probability of event p with respect to time. If in addition the process is stationary, the rate of events is constant and equation (2) can be simplified, since the first derivative of a stationary process is independent of the process itself, and formula (2) becomes:

$$\nu(x) = f(x)\int_0^\infty f(\dot{x})\dot{x}d\dot{x} \qquad (3)$$

For a Normal process, the theoretical rate of events can be found by substitution of the normal distribution into formula (3):

$$\nu(x) = \frac{1}{2\pi}\left(\frac{\sigma_{\dot{x}}}{\sigma_x}\right)\exp\left(-\frac{x^2}{2\sigma_x^2}\right) = \frac{1}{T_Z}\exp\left(-\frac{x^2}{2\sigma_x^2}\right) \qquad (4)$$

In formula (4), $\sigma_{\dot{x}}$ is the standard deviation of the time derivative of the process and T_Z is the upcrossing period of the process. Using the linear and nonlinear processes of the example case, upcrossing rate has been built for different levels by upcrossing counting. Figure 6 shows the results for both processes.

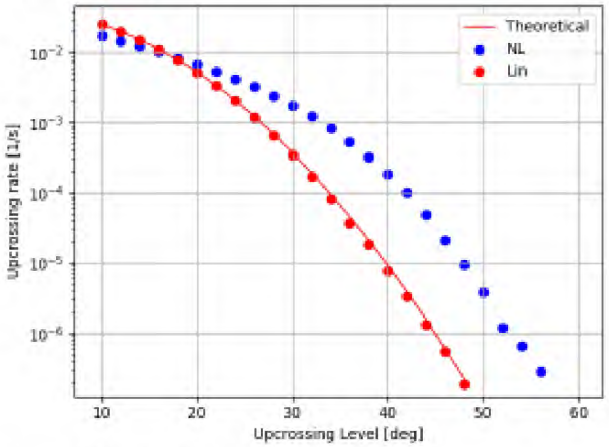

Figure 6: Upcrossing rate for linear and nonlinear processes

The upcrossing rate for the linear process is very close to the theoretical upcrossing rate (equation (4)). This result was expected, since we have seen in section 3 that the linear process follows a Normal distribution and the theoretical rate (equation (4)) was derived under the assumption of Normal distribution.

5. TIME TO FIRST EVENT DISTRIBUTION

The time to first event can be considered as the time to first upcrossing. Since an upcrossing may occur at any instant of time, the time to first event is a random variable. In reliability engineering, time to first event statistics are used, and the exponential distribution is the only distribution used to model this random variable. The exponential distribution is derived under the assumption of the independence of events. The probability density function assuming an

exponential distribution for an exposure time T and failure rate λ_x related to an upcrossing level x is given by equation (5):

$$f_x(T) = \lambda_x \exp(-\lambda_x * T) \quad (5)$$

Using both processes described in section 2, a sample of intervals before the first upcrossing has been populated. To ensure the independence of events, the time to failure was measured from the beginning of the simulation up to the instant when the failure level is passed, afterwards the simulation was stopped and restarted from the beginning for another seed in the same sea conditions.

For a given level, the time to first event (also called time to failure) was determined as the mean of the thousand time to failure obtained from each simulation. Obviously, there are some cases where the time series did not crossed the failure level. If these cases are not taken into account, the mean time to failure will be biased.

To correct such a bias a censoring procedure was used. The censoring procedure used in this work consisted to link the case in which no upcrossing occurs with those where there was an upcrossing. This lead to have in one hand time to failure greater than the length of record in some cases, and on another hand the reduction of the number of the sample. Results for a failure level of 20 degrees are shown in Figure 7 in term of exceedance probability.

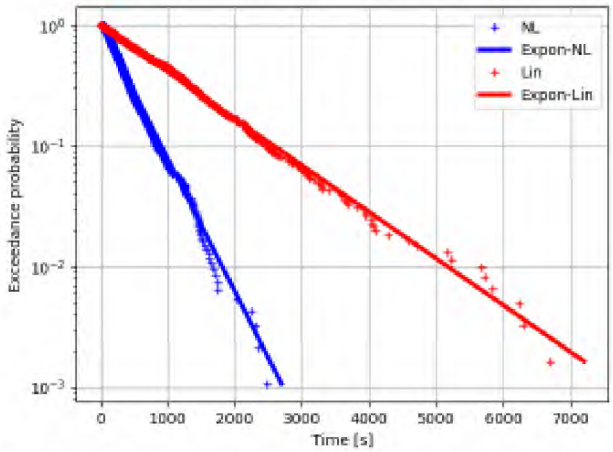

Figure 7: Time before first event distribution for linear and nonlinear processes – 20 degrees failure level.

Both linear and nonlinear processes are very close to the theoretical distribution. In addition, a Pearson chi-square goodness of fit test was performed for both distributions. The results of the tests are 0.93 for the linear process and 0.92 for the nonlinear process. The tests show that the fit are good for both processes since the probability are well above the accepted significance value of 0.05 assuming a confidence level of 95%. Other levels have been tested and the results were very good, and this confirm that the independence between events are respected and the time to first event are distributed following an exponential distribution. Note that in the current stage of development of the SGISC the time to first event is the standard method used in Level 3 (also called direct stability assessment) in full probabilistic assessment and in the probabilistic assessment in design situation as described in SDC 6/WP.6 – Annex 1.

6. TIME BETWEEN EVENTS DISTRIBUTION

An estimate of rate of events can also be evaluated from statistics of time between events. It's assumed that time between failures follows an exponential distribution. Therefore the probability density function of time between events can be described by formula (5) substituting the failure rate of the time before event λ_x by the failure rate of the time between events δ_x.

Using the dataset described in section 2, a sample of time between crossings has been populated for the linear and nonlinear processes. Results for a failure level of 20 degrees are shown in Figure 8.

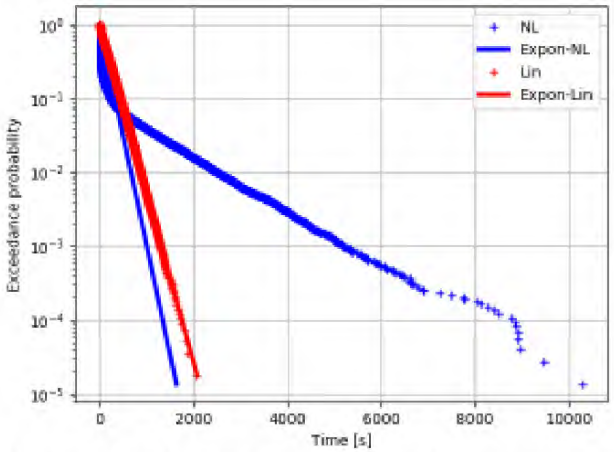

Figure 8: Time between events distribution for linear and nonlinear processes – 20 degrees failure level.

The linear process shows a good agreement with the theoretical distribution and this was confirmed also by a Pearson chi-square goodness of fit test which provided a result of 0.62 > 0.05 (for 95% confidence level). While for the nonlinear process, the computed distribution and the theoretical

distribution are different; in addition the computed distribution failed the Pearson chi-square goodness of fit test, since the probability is below the accepted significant value (0.00156 < 0.05), and therefore the hypothesis of exponential distribution is not supported by observed data. The most important condition is the independence of upcrossing.

Looking into the time series for the crossing level of 20 degrees, using the nonlinear process, most of upcrossings are clustered and there are many cases where neighboring periods have upcrossings.

7. CYCLE AMPLITUDES DISTRIBUTION

The cycle amplitudes distribution is built by determining and counting for example the greatest positive peak in each cycle. Therefore, secondary peaks are not taken into account.

Figure 9 shows an example for the linear process of the peaks taken into account to build the cycle amplitude distribution.

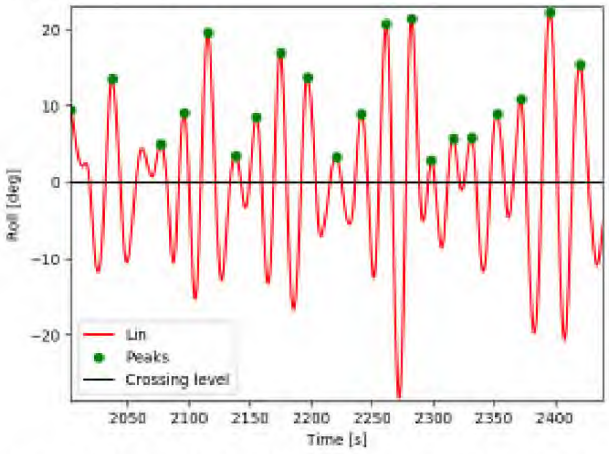

Figure 9: Example of identified peaks to build cycle amplitudes distribution for the linear process.

It's known that for a Normal process (linear process) having a narrow bandwidth spectrum, the distribution of cycle amplitudes is a Rayleigh distribution. The probability density function f_a of a Rayleigh distribution is given by:

$$f_a(x) = \frac{x}{\sigma_x^2} * \exp\left(-\frac{1}{2}\left(\frac{x}{\sigma_x}\right)^2\right) \qquad (6)$$

Using both processes of our example case, an upcrossing analysis has been performed to derive cycle amplitude distribution. The results of these analysis are shown in Figure 10.

As expected, the distribution for the linear process follows very the theoretical distribution, and the result of a Pearson chi-square goodness of fit test (0.94 > 0.05) confirmed also this result. We can also observe that distribution of peaks of the nonlinear process are not Rayleigh distributed. An explanation could be that the peaks determined for each cycle are not always independent.

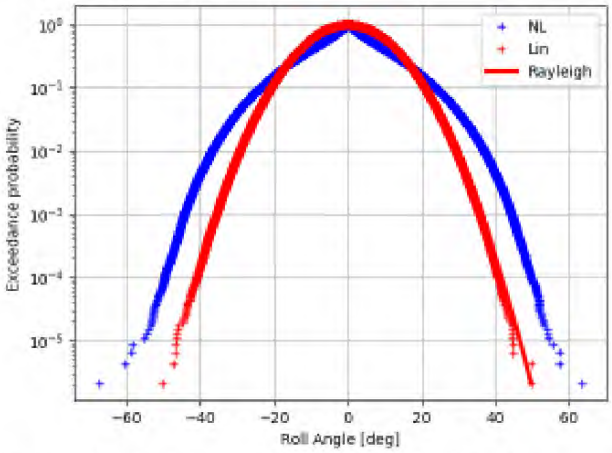

Figure 10: Cycle amplitudes distribution for linear and nonlinear processes.

8. MAXIMUM OVER A DURATION DISTRIBUTION

The maximum over a duration distribution or block maxima method consists of dividing the observation period into none overlapping independent blocks of equal size and restricts the attention to the maximum observation in each block. For a Normal process, the theoretical distribution for the maximum over a duration is given by:

$$F_T(x) = \left[1 - \exp\left(-\frac{1}{2}\left(\frac{x}{\sigma_x}\right)^2\right)\right]^{\frac{T}{T_Z}} \qquad (7)$$

In equation (7), T/T_Z represents the number of upcrossing cycles contained in the period T (block length). When the number of cycles is large enough (that means mathematically tends to infinity) the equation (7) becomes:

$$F_T(x) = \exp\left[-\frac{T}{T_Z} * \exp\left(-\frac{1}{2}\left(\frac{x}{\sigma_x}\right)^2\right)\right] \qquad (8)$$

Using both processes of our example case, for each simulation (with a duration of 3 hours), the maximum value of this 3 hours roll time series has been determined and the exceedance probability based on these 3 hours maxima is built. The results of these calculations are shown in Figure 11.

The results for the linear process are very close to theoretical distribution as expected. A Pearson chi-square goodness of fit test was done and the

results (0.54 > 0.05) confirmed also that the fitted distribution is supported by the data.

The maximum over a duration distribution can be considered as the most comprehensive definition with regards to design criteria. The final aim of short term probabilistic approach is to get this distribution.

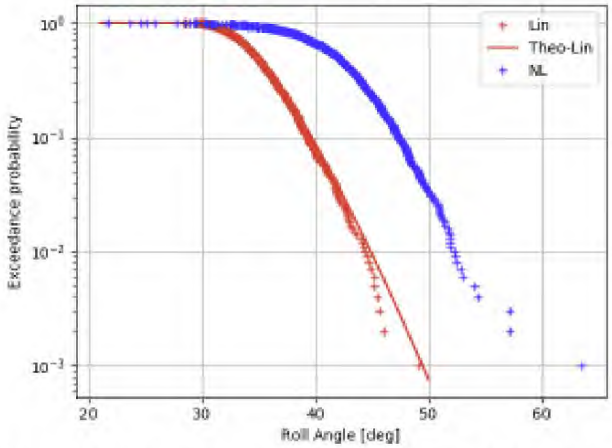

Figure 11: 3h maxima block exceedance probability for linear and nonlinear processes.

9. LINK BETWEEN DISTRIBUTIONS

This section describes the links between the different distributions defined from section 3 to section 8. The derivation of the distributions presented from sections 3 to 8, were not free of assumptions and jumping from one statistic to other might require also some assumptions among those: stationarity of the process (meaning that the conditions during the exposure time under assessment can be considered unchanged), the process is differentiable (meaning that the derivative of the process exists), and the events are independent and identically distributed.

Upcrossing rate vs maximum over a duration

Using the upcrossing rate ν, and assuming independent upcrossings and a Poisson process, the exceedance probability of the maximum over a duration could be computed using the formula (9):

$$F_T(x) = 1 - \exp(-\nu(x) * T) \qquad (9)$$

Using the results obtained in section 4, the exceedance probability over a duration of 3 hours has been computed using upcrossing rate for both processes and the results compared to those of section 8. The results of this comparison are shown in Figure 12.

From Figure 12, one can observe that the linear process results are very close to the reference (Max-Lin in Figure 12) for almost all roll angle. While for the nonlinear process, there are some differences below 44 degrees between the reference case (Max-NL) and the results obtained using upcrossing rate. These differences could be explained by the fact that the assumptions of independence of upcrossings is not verified for the nonlinear process below 44 degrees.

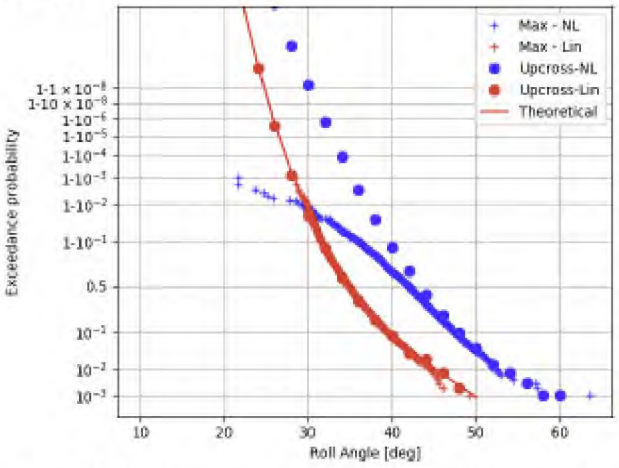

Figure 12: Maximum over a duration (3h) using upcrossing rate for linear and nonlinear processes.

Time to first even vs maximum over a duration

Using the time to first event failure rate λ, and assuming independent upcrossings and a Poisson process, the exceedance probability of the maximum over a duration could be computed using the following formula:

$$F_T(x) = 1 - \exp(-\lambda(x) * T) \qquad (10)$$

Using the results obtained in section 5, the exceedance probability over a duration of 3 hours has been computed using the time to first event failure rate for both processes. The results are shown in Figure 13.

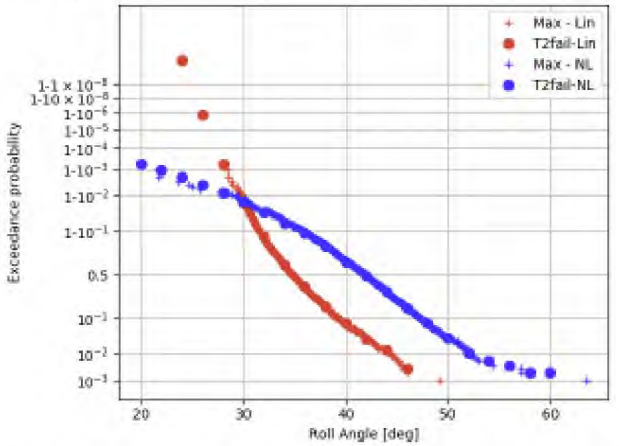

Figure 13: Maximum over a duration (3h) using time to first event for linear and nonlinear processes.

From results in Figure 13, one can observe that the results using time to first event for both linear and nonlinear processes are in agreement with the reference data (Max-Lin and Max-NL). These results are not surprising since independence of events is enforced during the construction of the time to first event for both processes.

Time between events vs upcrossing rate

Upcrossing rate (average number of upcrossings per unit of time) is obtained by counting the number of upcrossings above a given threshold, while time between events failure rate (inverse of the average time between upcrossings) is obtained by counting directly the time between upcrossings. Using the results obtained in section 4 (upcrossing rate distribution) and section 6 (time between events distribution), the rate of events obtained from upcrossing counting and time between events counting are compared and the results are shown in Figure 14.

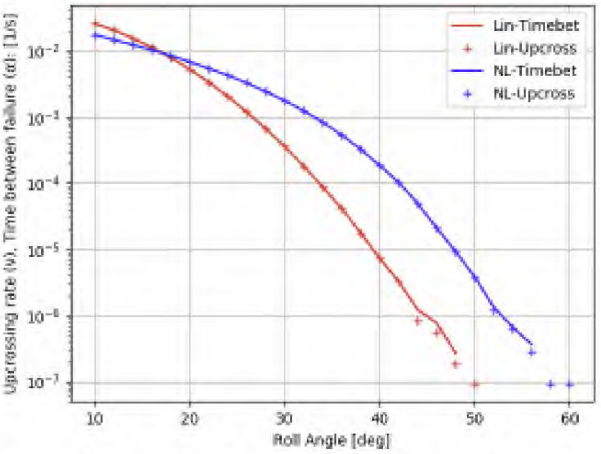

Figure 14: Comparison between upcrossing rate and time between events rate for linear and nonlinear processes.

One can observe that for both processes, the failure rate obtained from upcrossing and time between events are almost identical especially when the number of events are large. Therefore, the comments made on comparison between upcrossing rate and maximum over a duration are also valid for the comparison between time between events and maximum over a duration.

Cycle amplitudes distribution vs maximum over a duration

Using distribution of cycle amplitudes described in section 7, and assuming independent peaks, and a fixed upcrossing period, the probability for the maximum over a duration could be computed using the formula (7). Using the results obtained in section 7, the exceedance probability over a duration of 3h has been computed using the cycle amplitudes distribution for both processes and compared to the results obtained in section 8, the results of these comparisons are shown in Figure 15.

The results presented in Figure 15 show that for the linear process the exceedance probability obtained using cycle amplitudes distribution (Lin in Figure 15) follow very well the reference for linear process (Max-Lin in Figure 15). While for the nonlinear process, there are some discrepancies between the results obtained from cycle amplitudes distribution (NL in Figure 15) and the reference nonlinear case (Max-NL in Figure 15) when the roll angle is smaller than 44 deg.

These discrepancies are due to the independence between events condition which is not fulfilled below 44 degrees for the nonlinear process.

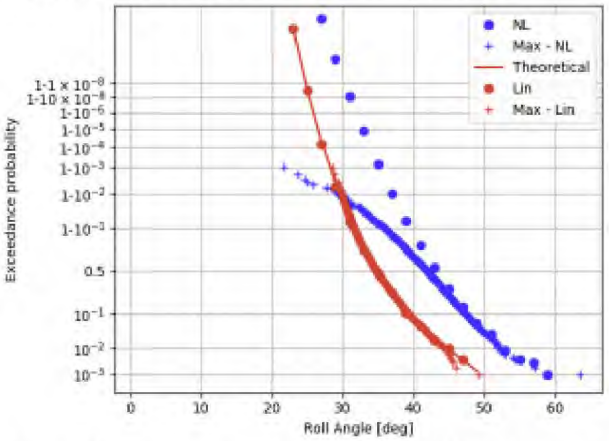

Figure 15: Maximum over a duration (3h) using cycle amplitudes distribution for linear and nonlinear processes.

Instantaneous value distribution vs upcrossing rate

The link between these two distributions is given by First Order Reliability Method (FORM). The statistical distribution of nonlinear ship responses can be estimated using FORM method, well known from structural reliability problems. One of the main result of FORM approach is the mean upcrossing rate of the process (roll motion for example) together with the most probable waves scenarios leading to the specified maximum roll angle for example.

Within FORM approach the mean upcrossing rate can be written according to Jensen and Capul (2006) using the FORM reliability index β_{FORM} as:

$$\nu(x) = \frac{1}{T_Z}\exp\left(-\frac{1}{2}\beta_{FORM}^2\right) \qquad (11)$$

The instantaneous value distribution is related to the FORM reliability index (β_{FORM}) by the following approximated relation:

$$F_i \approx \phi(\beta_{FORM}) \quad (12)$$

Since computing the reliability index (β_{FORM}) is time consuming, values of β_{FORM} have been selected directly from the instantaneous value distribution computed in section 3 for both linear and nonlinear processes as shown in Figure 16.

Having these reliability indexes, the upcrossing rate with FORM approach have been computed and the results are shown in Figure 17. From Figure 17, one can see that the upcrossing rate computed for the linear process using FORM approach are very close to those obtained using the theoretical formula (11).

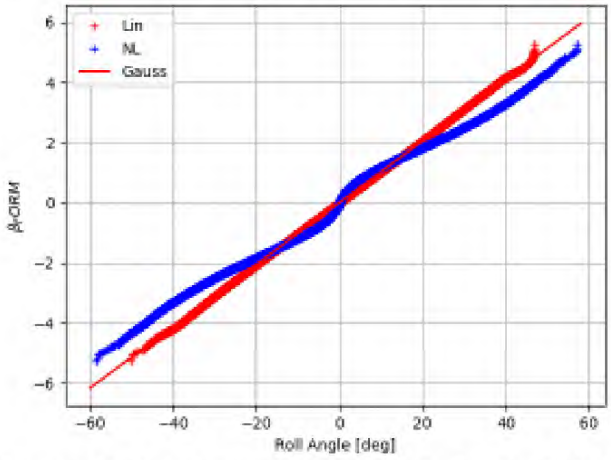

Figure 16: Instantaneous values distribution in FORM approach for linear and nonlinear processes.

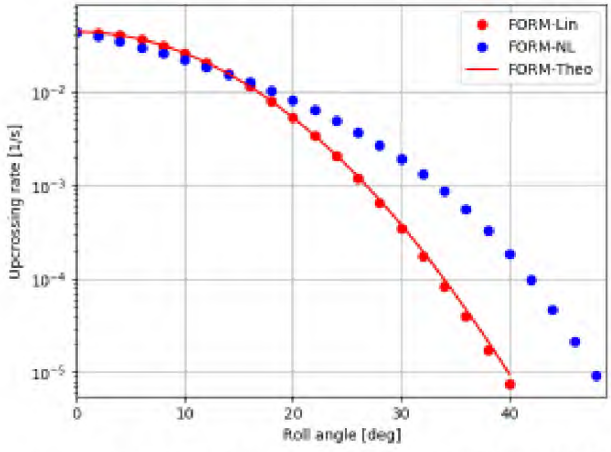

Figure 17: Upcrossing rate distribution using FORM approach for linear and nonlinear processes.

In addition, a comparison between the upcrossing rates obtained using FORM approach and upcrossing rates obtained using upcrossing counting (as described in section 3) has been carried out for both processes.

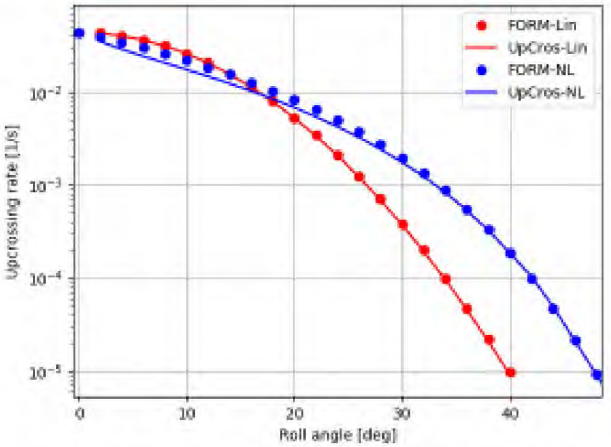

Figure 18: Comparison between upcrossing rates obtained from upcrossing counting and those from FORM approach for linear and nonlinear processes.

The results of this comparison are shown in Figure 18. From Figure 18 we can notice that for the linear process the two results are identical and there are some differences for the nonlinear process especially at lower roll angles.

10. INDEPENDENCE OF EVENTS ASSUMPTION

We have seen that independence of events is one of the most important condition to fulfill when using these different statistics.

Nonlinear process case

For example at 20 degrees roll angle using the nonlinear process, we have seen that most of upcrossings (for example for upcrossings counting, time between events, and cycle amplitudes) are clustered. Consequently there are many cases where neighboring periods have upcrossings as shown in Figure 19.

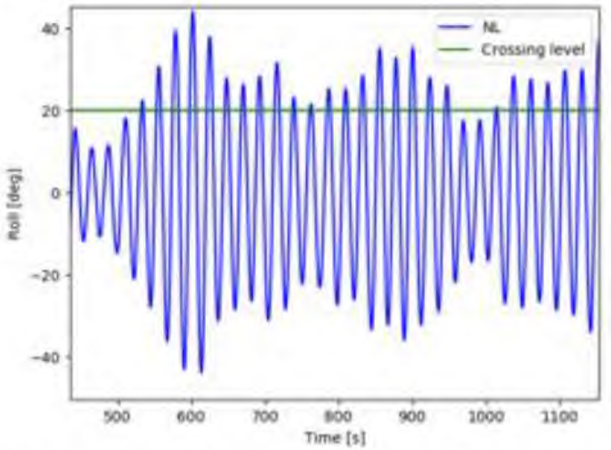

Figure 19: Time series of nonlinear process; 20 degrees upcrossing level.

Declustering the data could be a potential way to overcome this issue and a technique for declustering could be to use the envelope approach as described in Campbell and Belenky (2010).

Linear process case

For linear process i.e. Normal process, the autocorrelation function provides all information about dependence. This dependence has a limited duration, and the time it takes the autocorrelation function to drop below a given level is often used as a measure of this dependence. Using the linear process of the example case, the autocorrelation function has been computed and the result is shown in Figure 20. If the level is set to 0.05, it can be seen from Figure 20 that it takes about 50 seconds for this autocorrelation to die out.

To confirm this result, an assessment of time between events at 5 degrees has been computed and the results are shown in Figure 21.

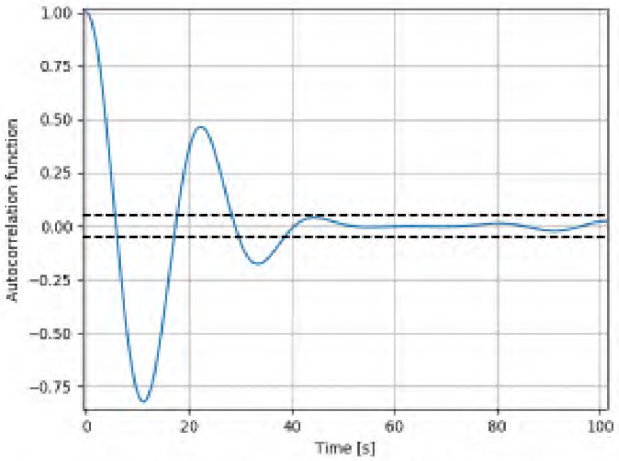

Figure 20: Autocorrelation function for the linear process.

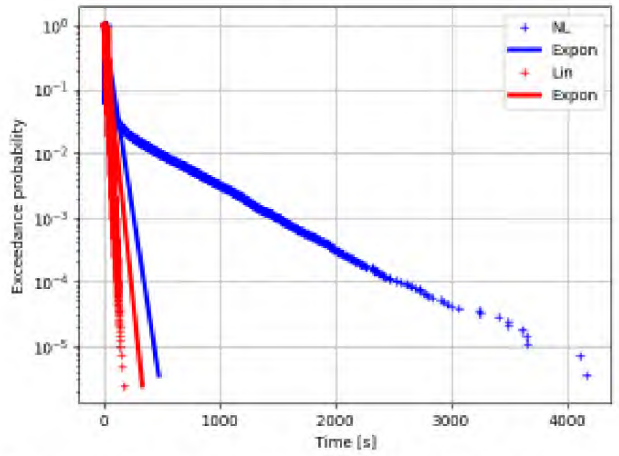

Figure 21: Time between events distribution for 5 degrees failure level for linear and nonlinear processes.

From Figure 21, one can observe that both processes do not show agreement with the theoretical distribution. In fact, a Pearson chi-square goodness of fit test (with the result of 0.0012 for the linear process and 0.00068 for the nonlinear process) rejects the exponential distribution based on time between events for 5 degrees level crossing. The theoretical distribution did not match the observed data for linear process because the observed data are clustered (for the upcrossing level of 5 degrees) and the independence of upcrossings are no longer guaranteed. This information is confirm also using autocorrelation function, since the mean time between events for 5 degrees upcrossing level is 38.6 seconds < 50 seconds (the required time to autocorrelation function to cross 5% level of significance (dashed black line in Figure 20)).

11. CONCLUSIONS

The difficulties to evaluate the probability of large roll angles are related to both the rarity of the event and the nonlinearity of the dynamical system describing the motion of a ship. One solution to overcome this issue is to use probabilistic or statistical techniques.

In summary this work focused on the review of existing probabilistic methods of evaluating dynamic stability using a dataset originated from numerical simulation. The different statistical distributions under these short term methodologies have been revisited and tested on two datasets consisting on a linear process and a nonlinear process. We have seen that these distributions under some assumptions are connected. Figure 22 presents the link between these different distributions.

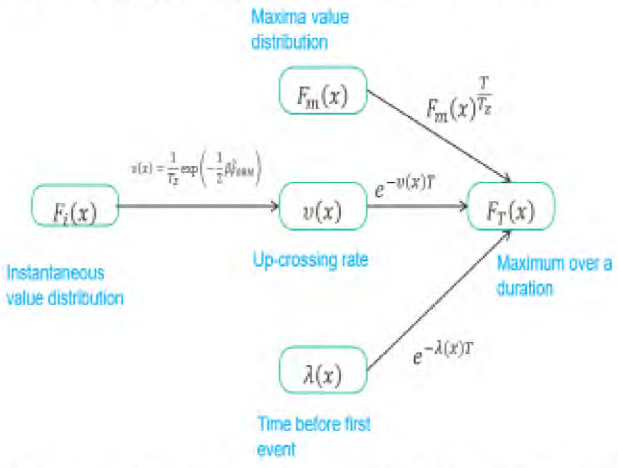

Figure 22: Overview of statistical distributions and their different links.

In Figure 22 the middle branch represents the FORM approach, a method widely used in structure reliability problems. This approach has been applied on dynamic stability problems. Jensen et al. (2017) applied this method for the statistical prediction of parametric roll. Choi et al. (2017) applied the FORM approach to analyze the stability of the ship under dead ship condition. Jensen (2007) applied FORM method to estimate extreme nonlinear roll motions.

One of the most important assumption behind the different probabilistic approaches is the independence of the events. The independence is not always guaranteed for the upcrossing of general stochastic process. Stochastic processes, such as roll angle or wave elevation for example have some inertia. Therefore, the instantaneous value of the process cannot change abruptly.

At the current stage of development of SGISC, the standard method in direct stability assessment is based on time to failure using the time to first event approach. We have seen that, we can achieve the same results using other statistical approaches if the assumptions behind these methodologies are verified.

ACKNOWLEDGEMENT

The author wish to thank Quentin Derbanne and Guillaume De Hauteclocque of Bureau Veritas for their guidance and their support for the investigation and compilation of these approaches.

The present study was partly supported by the Cooperative Research Ships (CRS) under the Direct Dynamic Stability Assessment (DYNASTY) Working Group.

REFERENCES

Campbell, B., Belenky, V., 2010, "Assessment of Short-Term Risk with Monte Carlo Method", Proceedings of the 11th International Ship Stability Workshop

Choi, J., Jensen, J., J., Kristensen, H., O., Nielsen, U., D., Erichsen, H., 2017, "Intact Stability Analysis of Dead Ship Conditions using FORM", *Journal of Ship Research*, Vol. 61, No. 3, pp. 167-176

IMO SDC 6/WP6 2019, "Report of the Expert's Group", 7 February

Jensen, J., J., 2017, "Efficient Estimation of Extreme Non-linear Roll Motions using the First-order Reliability Method (FORM)", *J. Mar. Sci. Technol.* 12(4), pp. 191-202

Jensen, J. J., Capul, J., 2006, "Extreme Response Predictions for Jack-up Units in Second Order Stochastic Waves by FORM", *Probabilistic Engineering Mechanics*, Vol. 21, No 4

Jensen J., J., Choi, J., Nielsen, U., D., 2017, "Statistical Prediction of Parametric Roll using FORM", *Ocean Engineering* 144, pp. 235-242

Wandji, C., 2018, "Investigation on IMO Second Level Vulnerability Criteria of Parametric Rolling", Proceedings of 13th International Conference on the Stability of Ships and Ocean Vehicles, (STAB2018), pp. 202-212

Wandji, C., Corrignan, P., 2012, "Test Application of Second Generation IMO Intact Stability Criteria on a Large Sample of Ships", Proceedings of 11th International Conference on the Stability of Ships and Ocean Vehicles, (STAB2012), pp. 129-139